

Revista Facultad de Ingeniería Universidad de Antioquia

ISSN: 0120-6230 ISSN: 2422-2844

Facultad de Ingeniería, Universidad de Antioquia

Murcia-Mesa, Julie Joseane; Patiño-Castillo, Ceidy Geraldine; Rojas-Sarmiento, Hugo Alfonso; Navío-Santos, José Antonio; Hidalgo-López, María del Carmen; Angel-Botero, Alberto Photocatalytic treatment based on TiO2 for a coal mining drainage\* \*\*

Revista Facultad de Ingeniería Universidad de Antioquia, no. 107, 2023, April-June, pp. 88-101

Facultad de Ingeniería, Universidad de Antioquia

DOI: https://doi.org/10.17533/udea.redin.20211063

Available in: https://www.redalyc.org/articulo.oa?id=43075471008



Complete issue

More information about this article

Journal's webpage in redalyc.org



Scientific Information System Redalyc

Network of Scientific Journals from Latin America and the Caribbean, Spain and Portugal

Project academic non-profit, developed under the open access initiative



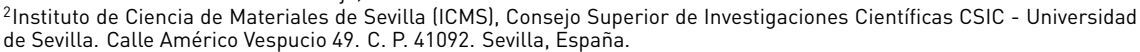
# Photocatalytic treatment based on TiO<sub>2</sub> for a coal mining drainage



Tratamiento fotocatalítico basado en TiO<sub>2</sub> para un drenaje de minería de carbón

Julie Joseane Murcia-Mesa (D), Ceidy Geraldine Patiño-Castillo (D)\*, Hugo Alfonso Rojas-Sarmiento (D), Antonio Navío-Santos (D), María del Carmen Hidalgo-López (D), Alberto Ángel-Botero (D)

<sup>1</sup>Grupo de Catálisis, Escuela de Ciencias Químicas, Universidad Pedagógica y Tecnológica de Colombia. Avenida Central del Norte 39- 115. C. P. 150007. Tunja, Colombia.



<sup>3</sup>Grupo de Investigación CITESA, Instituto de Recursos Minero Energéticos, Universidad Pedagógica y Tecnológica de Colombia. Calle 4 A Sur # 15-134. Sogamoso, Colombia.



#### **CITE THIS ARTICLE AS:**

J. J. Murcia-Mesa, C. G. Patiño-Castillo, H. A. Rojas-Sarmiento, A. Navío-Santos, M. C. Hidalgo-López and A. Ángel-Botero."Photocatalytic treatment based on TiO<sub>2</sub> for a coal mining drainages", *Revista Facultad de Ingeniería Universidad de Antioquia*, no. 107, pp. 88-101, Apr-Jun 2023. [Online]. Available: https://www.doi.org/10.17533/udea.redin.20211063

#### **ARTICLE INFO:**

Received: January 25, 2021 Accepted: October 13, 2021 Available online: October 13, 2021

#### **KEYWORDS:**

Photocatalysis; pollutants; real sample; treatment

Fotocatálisis; contaminantes; muestra real; tratamiento

ABSTRACT: The aim of the present work was to evaluate the effectiveness of a heterogeneous photocatalyst based on  $TiO_2$  in the treatment of coal mining drainage which contains a variety of heavy metals and high concentration sulfates and sulfides. The photocatalytic behavior of the commercial reference Sigma Aldrich and the different materials synthesized using the Sol-gel methodology with surface modifications using sulfation and fluorination processes were analyzed. To find a possible correlation between the physicochemical properties of photocatalysts and their behavior, a characterization was carried out using X-Ray Diffraction (XRD), X-Ray Fluorescence spectrometry (XRF), Fourier transform infrared spectroscopy (FT-IR), UV-Vis diffuse reflectance Spectra (UV-Vis DRS),  $N_2$  physisorption, X-ray photoelectron spectroscopy (XPS), and particle size analysis. Results indicated that the modification of the  $TiO_2$ prepared in the laboratory using sulfation and fluorination allowed the successful control of the physicochemical properties of this oxide. However, commercial  $TiO_2$  showed the greatest effectiveness in removing metals such as: Fe, Cu, Cr, and As after a photocatalytic reaction for a maximum of 1 hour under continuous nitrogen flow and a light intensity of 120  $W/m^2$ .

RESUMEN: El objetivo del presente trabajo fue evaluar la efectividad de la fotocatálisis heterogénea basada en  $TiO_2$  en el tratamiento de un drenaje de la minería de carbón, contaminado con una variedad de metales pesados y altas concentraciones de sulfatos y sulfuros. Se analizó el comportamiento fotocatalítico de la referencia comercial (Sigma Aldrich) y de los distintos materiales sintetizados por la metodología Sol-gel, con modificaciones en superficie por procesos de sulfatación y fluorización. Para hallar una posible correlación entre las propiedades físicoquímicas de los fotocatalizadores y su comportamiento, se realizó una amplia caracterización usando técnicas de análisis instrumental como Difracción de rayos X (DRX), Fluorescencia de rayos X (FRX), Espectroscopia infrarroja con transformada de Fourier (FT-IR), Espectrofotometría UV-Vis de reflectancia Difusa (UV-Vis DRS), Fisisorción de  $N_2$ , Espectroscopia fotoelectrónica de rayos X y granulometría. En general se encontró que la modificación del  $TiO_2$  preparado en el laboratorio por sulfatación y fluorización permitió el control exitoso de las propiedades físicoquímicas de este óxido. Sin embargo, el  $TiO_2$  comercial presentó la mayor efectividad en la remoción de metales como: Fe, Cu, Cr y As, todo ello empleando un máximo de 1 hora de reacción fotocatalítica, bajo flujo continuo de nitrógeno y una intensidad de luz de 120  $W/m^2$ .

\* Corresponding author: Ceidy Geraldine Patiño-Castillo E-mail: ceidy.patino@uptc.edu.co ISSN 0120-6230 e-ISSN 2422-2844





## 1. Introduction

Water pollution from coal mining mainly occurs during the exploitation stage, in which the mineral comes into contact with natural water sources. These mineral wastes include metal sulfides [pyrite  $(FeS_2)$ , pyrrhotite (Fe1-xS), chalcocite  $(Cu_2S)$ , galena (PbS), etc.], which are involved in oxidation reactions and leaching processes [1, 2]. As a result of these reactions, acids drainages and the presence of heavy metals in solution have a negative impact on the environment [3].

Different methods for the treatment of this type of drainages have been developed, among which membrane filtration (electrodialysis, reverse osmosis, nanofiltration, and ultrafiltration), ion exchange, adsorption (activated carbon and carbon nanotubes), chemical precipitation, electrocoagulation, coagulation-flocculation, electroflocculation, and flotation [4]. However, in certain cases, this type of technology is ineffective due to the high toxicity of the drainage to be treated or due to the high operating cost. In addition, the formation of sludge and waste byproducts created from these treatment processes requires subsequent treatment for appropriate disposal.

One of the most promising technologies for the treatment of polluted water are Photocatalysts based on  $TiO_2$  which has demonstrated to be highly effective in the degradation of organic contaminants and microbiology elimination without the generation of residual sludge or phototransformation of metal ions into species of less toxicity [4–7], hence its consideration as a non-selective technology. However, in most of the studies carried out on this subject, matrices prepared in the laboratory or synthetic waters are used, which vary in the effectiveness of the photocatalytic treatment due to the variety of organic and inorganic contaminants present in a real sample [5, 8].

The main objective of this study was to evaluate heterogeneous photocatalysis using  $TiO_2$  as an alternative in the treatment of coal mining drainage from the traditional extraction processes of one mine located in the department of Boyacá, Colombia, and to determine the best experimental conditions for photocatalysis.

## 2. Experimental section

#### 2.1 Synthesis of photocatalysts

The reference material used was  $TiO_2$  from Sigma Aldrich, which will be called  $TiO_2$  (Sigma) from now on, and another  $TiO_2$  prepared in the laboratory by following a variation of the Sol-gel method by controlled hydrolysis of titanium tetraisopropoxide (TTiP Aldrich 97%) in solution

with 1.6 M isopropanol and the addition of distilled water in a 1:1 ratio. The precipitate obtained was recovered by filtration and dried at 110 °C for 12 hours. Some part of this material was calcined at 650 °C for 2 hours with heating increments of 4 °C/min (Sq- $TiO_2$ ). The remaining quantity was subjected to surface modification processes by sulfation (S- $TiO_2$ ) and fluorination (F- $TiO_2$ ) to improve its physicochemical and optical properties [9] by being immersed in a 1.0 M of  $\mathrm{H_2SO_4}$  and 10.0 mM of NaF, respectively. In the case of fluoridation, the pH was adjusted to 3.0 using a 1.0 M HCl solution to maximize the absorption of fluorine ions on the surface of the photocatalyst [10]. These suspensions were kept under constant stirring for 1 hour, filtered, and dried at 110 °C for 12 hours. The product was then calcinated for 2 hours at 650 °C with heating increments of 4 °C/min [9].

#### 2.2 Characterization of the photocatalysts

The composition of the crystalline phases and the degree of crystallinity of the materials were studied using X-ray diffraction (XRD). An analysis was performed using a Philips PW1700 diffractometer and  $Cu(K\alpha)$  radiation. The diffractograms were obtained by making a continuous scan at an angle of 20 between 20 and 80°. The crystallite sizes of the Anatase phase were calculated using the position and width data of the main peak at 25.225° of the Anatase and the Scherrer equation. The width values were obtained by taking half of the height of the peaks and using the Voigt function to adjust the diffraction profiles.

The chemical composition of the photocatalysts was determined by X-ray Fluorescence Spectrometry [XRF], using an Axios sequential Panalytical spectrophotometer with a Rhodium anode as the radiation source. To carry out the measurements, the samples were supported on pads made with boric acid. Each sample was mixed with wax and pressed into the pads with a proportion of 10 Wt.%.

The qualitative analysis of the functional groups present in the photocatalysts was carried out using Fourier transform Infrared Spectroscopy (FT–IR). FT-IR was carried out using the ATR cell of a Thermo Scientific Nicolet iS50 FT-IR spectrometer using a range between 4000–1000  $cm^-1$ .

The light absorption properties of the samples were analyzed by Ultraviolet-Visible Diffuse Reflectance Spectrophotometry (DRS). A Varian model Cary 100 spectrophotometer was used and equipped with an integrating sphere using  ${\rm BaSO_4}$  as a reference. The band gap values of the photocatalysts were calculated with the Kubelka-Munk function F  $F(R\infty)$ , which relates the diffuse reflectance of the material with the adsorption and dispersion coefficients.

The surface area of the synthesized photocatalysts was determined by the Physisorption of  $N_2$ . A Micromeritics ASAP 2010 was used, and the Brunauer-Emmett-Teller method was selected. The measurements were carried out using nitrogen adsorption/desorption isotherms at 77 K. The weighed samples were previously degassed at 423 K for 1 h under vacuum and under a stream of dry  $N_2$ .

The surface composition of the samples was determined using X-ray Photoelectron Spectroscopy (XPS). A Leybold–Heraeus LHS-10 spectrometer was used with a constant energy step of 50 eV. The main chamber of the spectrometer was operated at a pressure of  $<2\times10^{-9}$  Torr and is equipped with an EA-200 MCD hemispherical electron analyzer with a dual X-ray source. The machine worked with the Al  $K\alpha$  line (hv = 1486.6 eV) at 120 W and 30 mA. In all experiments, the C 1s signal (284.6 eV) was used as a reference. The samples were degassed in the instrument pre-chamber at 423 K and a pressure of  $<2\times10^{-8}$  Torr to remove chemisorbed water.

Finally, the grain size of each material used was determined by granulometry. The materials were passed through a set of sieves with different openings (30, 40, 50, 100, and 200  $\mu m$ ).

## 2.3 Physicochemical analysis of coal mining drainage

The coal mining drainage samples were collected at the coordinates N:1125881; E 1134207; of a mine located in the municipality of Monguí, Colombia. The procedure for the collection, preservation, and physicochemical analysis of the samples was carried out in accordance with the measures established in the Standard Methods for the Examination of Water and Wastewater, [SM] [11]. The physicochemical parameters analyzed, the code corresponding to the selected method, and the equipment used are listed below.

pH was determined by the electrometric method (SM. 4500 H+ pH value-B.) using a pH meter from the SI Analytics Lab 850.

The phenol concentration was determined by the direct method using UV-Visible spectrophotometry (SM. 5530-D.) and a Themovision EV-300 spectrophotometer was used.

The concentration of Chlorides  $(\mathrm{Cl}^-)$  and Sulfates  $(\mathrm{SO}_4^{-2})$  was determined by using the ion chromatography method with chemical suppression of the conductivity of the eluent (SM. 4110-B.), using a 761 Compact IC Metrohm chromatograph and the METROSEP A SUPP column 5–150/4.0.

The sulfide concentration  $(S^{2-})$  was determined using the iodometric method (SM.  $4500 \, S^{2-} - F.$ ).

For the analysis of the concentrations of Cd, Cu, Cr, Fe, Ni, and Pb, a pretreatment of the samples was carried out by using a nitric acid digestion process (SM. 3030-E.). The samples destined to determine the concentration of As were digested with a mixture of nitric acid and sulfuric acid (SM. 3030 - G.). Once all the samples had been digested, their analysis was carried out using the Flame Atomic Absorption Spectrometry (air-acetylene) (SM. 3111-B.). The analysis of As was carried out using the hydride generation method (Atomic Absorption Spectroscopy) (SM. 3114-B.). A SHIMADZU AA-7000 series spectrophotometer with a dual flame-furnace system and hydride generator was used to determine concentrations after preparing a series of calibration curves generated from standard solutions of 1000 mg/L metal. These solutions were diluted to concentrations suggested by the instrument manufacturer manual.

Total organic carbon (TOC) was determined by the method (SM 5310 B), using a COT Multi N/C 2100, Analytikjena. The analysis of total suspended solids (SM. 2540-D.), settling solids (SM. 2540-F), acidity (SM. 2010- B.), alkalinity (SM. 2320-B.), calcium hardness (SM. 3500 - Ca D.), total hardness (SM. 2340-C.), turbidity (SM. 2130-B), and true color (SM. 2120-C.) were also performed.

### 2.4 Evaluation of the photocatalytic activity

The photocatalytic treatment system consisted of a 400ml pyrex "batch" type reactor covered with aluminum foil and protected with a Plexiglas® UV plate (transparent for wavelengths higher than 250 nm). The incident light source corresponded to an Osram Ultra-Vitalux 300W lamp (containing a radiation spectrum similar to the sun and a main emission line in the UVA range at 365 nm), which was previously calibrated for the system with the intensity of UV-Visible incident light on the suspension at  $120\ W/m^2$  using a Delta OHM HD 2102.2 photoradiometer.

The photocatalytic reactions were carried out by using the injection of a continuous flow of nitrogen (0.84 L/h) to guarantee a reduced atmosphere and with constant stirring in order to produce a homogeneous suspension of the photocatalyst in the solution. In each photocatalytic test, a 250 mL sample of the coal mining drainage was used in suspension with 1 g/L of the photocatalyst. This suspension was homogenized in ultrasound for 10 minutes and kept under stirring for a further 10 minutes in the dark in order to achieve an adsorption-desorption equilibrium. The conditions mentioned above also applied to the control reaction (without adding photocatalyst), which was carried out to determine the effect of light and the efficiency of the

process when a photocatalytic material is present.

For this study, different treatments (Blank,  $TiO_2$  (Sigma),  $Sg-TiO_2, S-TiO_2, F-TiO_2)$  were tested on the drainage derived from a single mine under the conditions previously described. The total time of the reactions was 5 hours, taking aliquots from the reactions after different times (1, 3, and 5 hours). Samples were recovered by filtration using 0.45  $\mu$ m Milipore Milex-HV hydrophilic PVDF filters. At the end of the reaction time, the solid photocatalyst was recovered using Whatman grade 1 paper filters.

All the reactions were carried out in duplicate, and the analysis of the monitored parameters (metals, anions, phenols, and TOC) were carried out in triplicate. This ensured the reproducibility of the results and the consistency of the information collected.

The determination of the percentage of removal of contaminants from the fluid phase, the initial concentrations (before treatment, Ci), and final concentrations (after treatment, Cf) of each sample were taken into account as indicated in Equation 1.

$$\%$$
 Remoción de la fase fluida  $= \frac{\mathrm{Ci} - \mathrm{Cf}}{\mathrm{Ci}} * 100$  (1)

#### 3. Results and discussion

#### 3.1 Characterization of photocatalysts

A summary of the characterization results is presented in Table 1. The different instrumental techniques used and the results obtained are escribed below.

#### X-Ray Diffraction (XRD)

The diffractograms obtained for the photocatalysts studied are presented in Figure 1. The Sq- $TiO_2$ photocatalyst presents the crystalline phases Anatase (JCPDS 00-001-0562) and Rutile (JCPDS 00-001- 1292), identified by their characteristic signals located at 25.25° and 27.32°, respectively. On the contrary, the commercial reference  $TiO_2$  (Sigma) and the materials modified by sulfation and fluoridation only present the Anatase crystalline phase in their structure. due to the protective effect of the fluoride and sulfate species that stabilized the oxide surface and inhibited the formation of the Rutile crystalline phase during the calcination process, as has been reported in different previous studies [9, 12]. Some authors have reported that the presence of the anatase phase is preferential in the  $TiO_2$  material and favors the photocatalytic process.

This occurs as a result of the fact that this phase presents

a higher degree of crystallinity, a lower recombination speed of the electron-hole pairs, higher energy in its band gap than rutile [12], and a higher active surface area and density of active sites available for the adsorption of substances [13–15].

The sizes of the Anatase crystal were calculated using the Scherrer equation. The results are shown in Figure 1 and demonstrate how the fluoridation and sulfation processes favored an increase in the size of the Anatase crystallite in relation to Sg- $TiO_2$  [9].

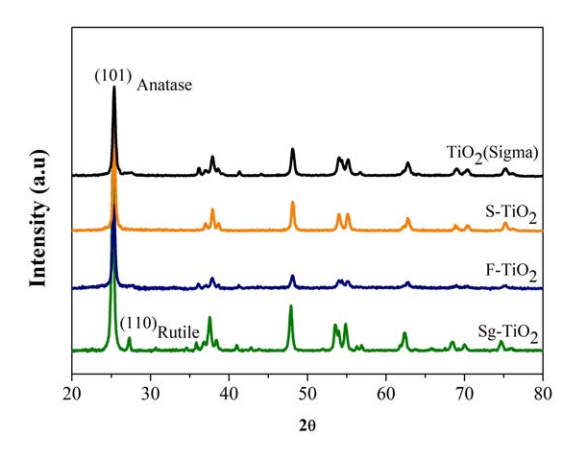


Figure 1 X-ray diffractograms for photocatalysts based on  $TiO_2$ 

#### X-ray Fluorescence Spectrometry (XRF

The chemical composition of the surface-modified materials was determined by XRF. The analysis revealed that a certain amount of S remained on the solid  $(S-TiO_2)$  after preparation. The sulfur content in sulfated material was 0.66 wt%, since as reported in other studies, this temperature is insufficient to completely eliminate the sulfate groups that remain anchored to the oxide surface and are only removed at temperatures above 700°C [16]. In the photocatalyst modified by fluoridation, no traces of Na were detected by XRF, and the remaining content of Clwas negligible (<0.02 wt. %); this residual chlorine can come from the HCl solution employed for pH stabilization, where some drops of this acid were added during the synthesis of  $F-TiO_2$  material.

#### Fourier transform infrared spectroscopy (FT-IR)

The functional groups present in the materials used and the type of hydroxyl groups were identified by FT-IR analysis. Figure 2 indicates the region of the IR spectrum in the range of 4000 to 2500  $\rm cm^{-1}$  of the IR spectrum. The band located at  $3698~\rm cm^{-1}$  indicates the presence of isolated OHD groups in all of the samples analyzed. Bands located at  $3385~\rm cm^{-1}$  and  $2915~\rm cm^{-1}$  are assigned to linked

Table 1	I Table 1 Cha	ractorization	recults of the	materials used
lable	i Tanie i Una	iracienzanon	resilles of the	materials usen

Photocatalyst	Anatase crystallite size	Band gap	Surface area SBET	Binding e	٠.	0/Ti	Grain size
	(DANATASE)		$\left(\mathbf{m}^2/\mathrm{g}\right)$	$Ti2P_{3/2}$	0 15		(µm)
$TiO_2$ (Sigma)	22	3.23	51	458.5	529.8	1.87	1.87
$Sg - TiO_2$	17	3.30	11	458.5	529.8	1.96	1.96
$F - TiO_2$	24	3.21	51	458.4	529.6	2.00	2.00
$S - TiO_2$	20	3.20	58	458.5	529.8	1.70	1.70

hydroxyl groups (Ti- OH) and adsorbed water  $(Ti-OH_2)$ , respectively [17, 18]. The intensity of the band attributed to the terminal group Ti-OH is higher in the spectrum of  $S-TiO_2$  materials; however, the intensity of the bands decreases after the addition of fluorine. This indicates that the  ${\bf F}^-$ ions can replace the  ${\bf OH}^-$  groups (Titanol groups) of  $TiO_2$ , modifying its surface. As it was reported by Torrents et al. [19], each fluorine substituted/adsorbed occupy  $0.33~{\rm nm}^2$  on the  $TiO_2$  surface, similar to Vohra et al. [20] have found that the 95% of Titanol groups are replaced by Fluorine ions in an interval pH value between 3 and 5, using a 10mM NaF solution as Fluorine precursor.

#### **UV-Vis Diffuse Reflectance Spectrophotometry (DRS)**

The light absorption properties of the photocatalysts used were analyzed by UV-Vis DRS. Figure 3 shows the spectra obtained for the studied materials. There is a characteristic absorption band of  $TiO_2$  between 200 and 400 nm. The Fluorized sample shows a slight displacement of the absorption band towards the visible region of the electromagnetic spectrum, which is due to the presence of fluoride ions on the surface of the titania [9].

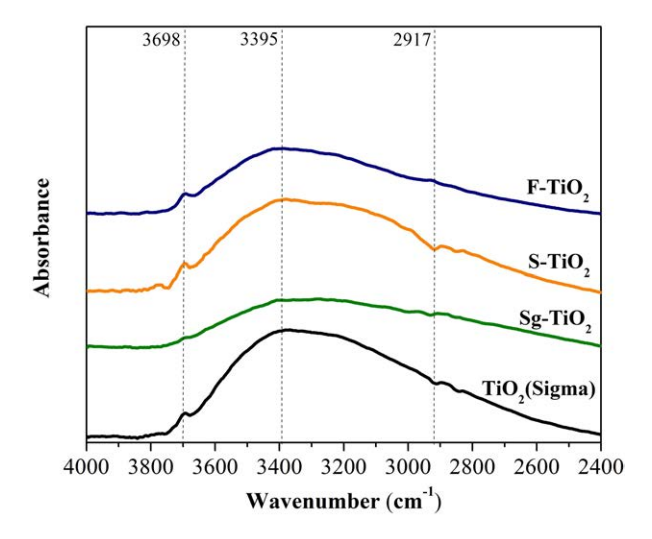


**Figure 2** FT-IR spectra of the analyzed photocatalysts in the region between 4000 and  $2400~{
m cm}^{-1}$ 

Following the Tandom and Gupta method, the band gap of

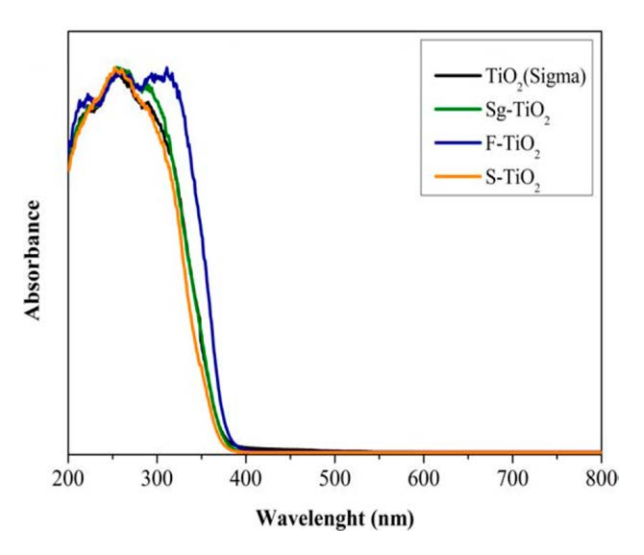


Figure 3 UV-Vis DRS spectra for the photocatalysts analyzed

each material used was found. The results are presented in Table 1. The modification in the oxide surface due to sulfation and fluoridation contributed to reducing the band gap of the  $TiO_2$  which approached the value of the band gap of the commercial reference  $TiO_2$  (Sigma).

#### **N2** physisorption

The specific surface area (SBET) of the photocatalysts used was determined using nitrogen physisorption and shown in Table 1. The  $TiO_2$  synthesized in the laboratory using the Sol-gel method resulted in a lower surface area (SBET), compared to the other materials. The lower SBET in the  $Sg-TiO_2$  can be due to the sintering of the particles during the calcination process. In the case of the modification by fluorination and sulfation, it was found to generate a protective effect on  $TiO_2$  surface, inhibiting the agglomeration of the particles.

#### X-ray Photoelectron Spectroscopy (XPS)

XPS made it possible to determine the binding energy of the synthesized materials and compare it with the commercial reference. In Figure 4a, the spectra in the Ti 2p region of the materials used in the study are shown. There were no significant modifications in the position of the signals located in their main component at binding

energies of  $458.6 \pm 0.1 \mathrm{eV}$ , which are characteristic of amount of these atoms in the photocatalyst.  $Ti^{4+}$  ions in the  $TiO_2$  crystal lattice.

The binding energy for the O1s region is located at  $529.8 \pm 0.2 \mathrm{eV}$ , which corresponds to surface oxygen atoms  $(O^{2-})$  in the crystal lattice of  $TiO_2$ . In Figure 4B, the peaks are asymmetric, with a slight increase towards bond energies higher than 531.3 eV, which are characteristic of the OH<sup>-</sup> groups.

On the other hand, the formation of free OH groups and oxygen vacancies have been corroborated in different studies which explain the dehydroxylation process during calcination at temperatures lower than 700°C. This is due to an excess of adsorbed protons leading to the creation of oxygen vacancies on the surface and promoting the separation of photogenerated charges, thus improving the photocatalytic efficiency of  $TiO_2$  through ion mobility and anions in solution [9].

In Table 1, a summary of the results for the binding energies in the region Ti 2p, O1s, and the atomic ratio O/Ti is shown. The O/Ti ratio calculated for the sulfated and fluorinated materials is lower than the stoichiometric value O/Ti = 2, thus indicating the presence of some oxygen vacancies on the semiconductor. The surface of the fluorinated  $TiO_2$  appears to favor the generation of free radicals •OH that create oxygen vacancies and increases the content of free hydroxyl groups, which is related by the estimation of O/Ti atomic ratio which reaches a maximum value of 2.0, suggesting the presence of surface hydroxyl groups after fluoridation. This result is supported in the study by T. Le et al. [21], who observed the growth of surface OHDgroups in their modified materials during the fluorination processes. These analyzes can be corroborated by the FT-IR results where a highly hydroxylated surface is observed for the  $S-TiO_2$  and  $F-TiO_2$  photocatalysts compared with bare  $Sg-TiO_2$ (Figure 2).

Figure 4c shows the deconvolution of the peaks corresponding to the O 1s region, carried out in the UNIFIT 2009 program for  $S-TiO_2$ . With regard to region F 1s of the fluorinated modified material that is presented in Figure 4d an analysis was performed and a main signal was found at a binding energy of  $684 \pm 0.18 \text{eV}$ . This is attributed to the fluoride groups present on the surface of the material ( $\equiv T - F$ ), which are formed by the ligand exchange reaction between the  $F^-$  and hydroxyl groups.

Using XPS, Cl, S, F, and Na were detected even after the calcination process at 650 ° C. These elements were found in 0.47%, 1.64%, 1.83%, and 2% quantities, respectively. In contrast, the XRF analysis showed no traces of Cl, F, and Na, which may be due to the low

Photocatalysis is a process that occurs on the surface of the semiconductor oxide making the size of the particle grain important in the photocatalytic process. This is significant because of the fact that the lifetime of an electron-hole pair is nanoseconds; hence very large particles can act as recombination centers. Furthermore, large surface areas are desirable in order to facilitate adsorption of the contaminant, while the absence of porosity allows the homogeneous illumination of the particles [22]. The granulometry results are presented in Table 1, where the  $TiO_2$  used as a commercial reference has a smaller grain size compared to the materials synthesized in the laboratory.

#### 3.2 Physicochemical analysis coal mining drainage

The study drainage from the coal mine was analyzed for its physicochemical composition and the main results obtained are summarized in Table 2. In general, it is evident that parameters such as pH, phenols, sulfates, sulfides, iron, lead, and TSS in the drainage exceed the maximum permissible limits required in article 10 of resolution 0631 of 2015.

issued by the Ministry of the Environment of Colombia. After taking into account the results obtained by the physicochemical analysis and considering the risks to the health of the population as a direct result of the discharge of these types of drainages into freshwater bodies, a photocatalytic treatment was applied to the real sample. Pollutants which are susceptible to be treated by this photocatalytic technique such as organic compounds (phenols) and inorganic compounds (ions and metals) were monitored. The results are described in detail in the following sections.

#### 3.3 Photocatalytic treatment

#### Removal of Fe, Cu, Cr and As

The monitoring of the changing concentrations of the metals Fe, Cu, Cr, and As during the photocatalytic treatment on the drainage from coal mining, is presented in Figure 5. During the control reaction carried out under UV-visible light and without the presence of a photocatalyst, there was a slight decrease in the concentration of these metals in the fluid phase, of about 3.63%. This indicates that the photoreduction reaction of the metals is slightly significant under UV-Vis light. On the other hand, as can be seen in these figures, the presence of a photocatalyst in the reaction medium leads to an increase in the effectiveness of the chemical reduction of metals on the surface of this material. The photochemical reduction process of these four metallic species occurs by

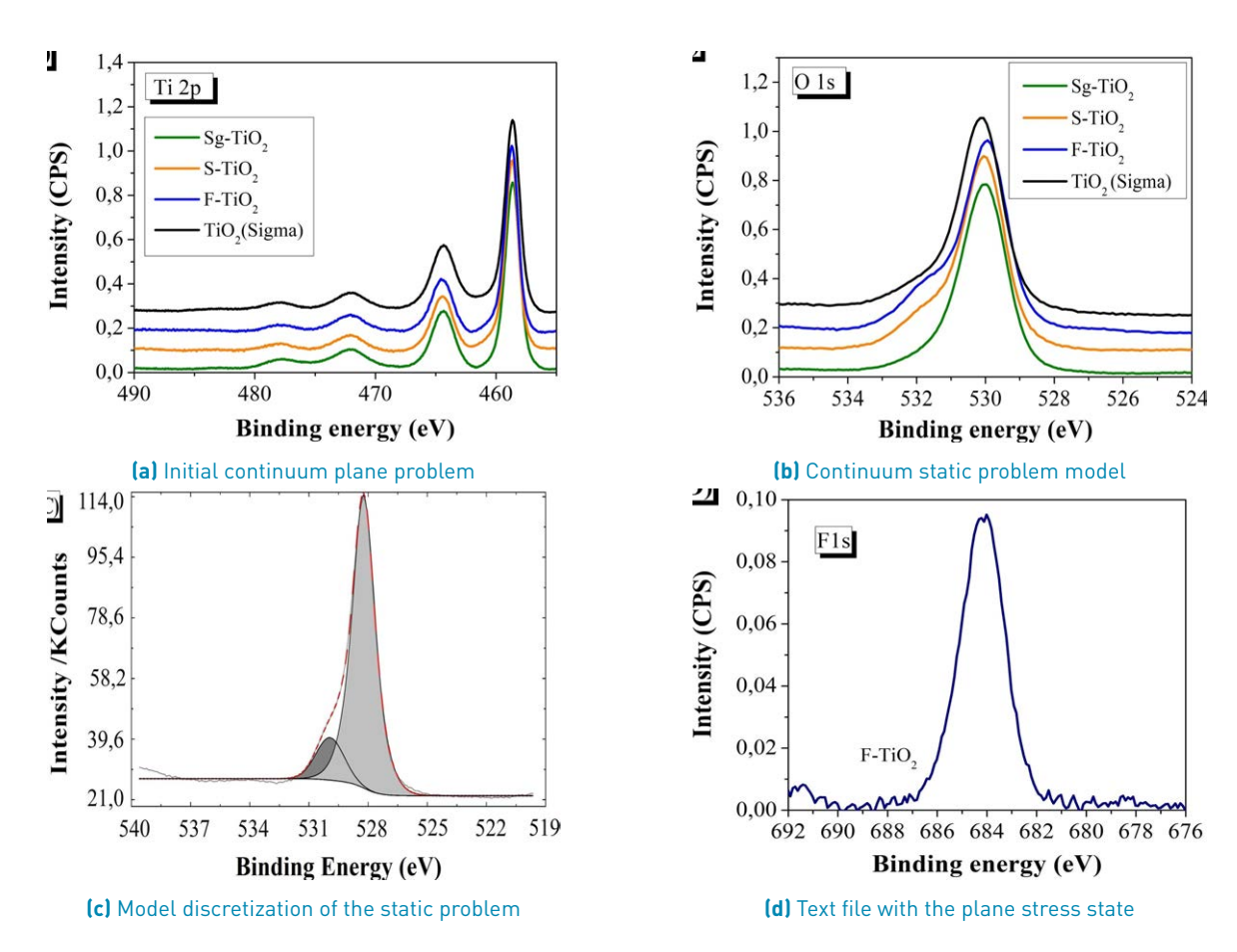


Figure 4 XPS spectra in the region (A) Ti 2p; (B) 01s; (C) Deconvolution of the XPS core level spectra of the 0 1s for S-Ti02; (D) F1s

Table 2 Physicochemical analysis of coal mine drains

Parameters	Units	Colombian regulations [23]	Mining drainage	
рН	Units	6-9	2.98	
Phenols	mg/L	0.2	8.74	
Chlorides	mg/L	500.0	0.002	
Sulfates	mg/L	1200.0	1598.37	
Sulfurs	mg/L	1.0	29.7	
Arsenic	mg/L	0.1	0.0073	
Cadmium	mg/L	0.05	<l.d< td=""></l.d<>	
Copper	mg/L	1.0	0.1172	
Chromium	mg/L	0.5	0.1525	
Iron	mg/L	2.0	49.712	
Nickel	mg/L	0.5	0.2808	
Lead	mg/L	0.2	0.8699	
Total suspended solids	mg/L	50.0	1774.50	
Sedimentable solids	mg/L	2.0	<0.10	
Acidity	mg/L	Analysis and reporting	605.0	
Alkalinity	mg/L	Analysis and reporting	0.57	
Calcium hardness	mg/L	Analysis and reporting	483.8	
Total hardness	mg/L	Analysis and reporting	859.7	
Turbidity	NTU	Analysis and reporting	655.0	
	436 nm	Analysis and reporting	2.25	
Real color	525 nm	Analysis and reporting	2.19	
	620 nm	Analysis and reporting	1.98	

L.D.: Limits of detection.

the action of the electrons of the conduction band (CB), and is described by Equation 2.

$$M^{n+} + TiO_2 (e^-BC) \to M^{(n-1)+}$$
 (2)

It is evident that in the presence of  $TiO_2$ , the concentration of the metals Fe, Cu, Cr, and As decreases significantly in the coal mining drainage. As a result, it is considered to be the best photocatalyst in the treatment of the mentioned drainage for the removal of these four heavy metals when compared with the other photocatalytic materials evaluated (Sg $-\mathrm{Ti}O_2$ , S $-\mathrm{Ti}O_2$  and F $-\mathrm{Ti}O_2$ )

It is important to note that for each of the photocatalysts evaluated, the concentration of Fe, Cu, Cr, and As in the fluid phase decreases significantly during the first hour of photocatalytic reaction. After this time, the concentration of these metals tends to increase, almost returning to the initial concentration of the metals in the coal mining drainage without treatment. This increase may be evidence of possible desorption of the metal from the surface of the semiconductor. Although "desorption" is mentioned, this would not be the most appropriate term to use because the phenomenon takes place during a photochemical reduction where the oxidation state of metals change from an oxidized state to its metallic state on the semiconductor surface [5, 7]. The correct thing to do is to propose a hypothesis of the observed behavior of the metals after the first hour of reaction which tends to undergo reoxidation; returning to their initial oxidation state, passing again from the solid phase of the semiconductor to the fluid phase of the reaction medium.

The metals are then subjected to reoxidization which is mainly due to the competition of H2O for the holes and/or hydroxyl radicals in such a way that the reduction of the metal is unfavorable and the initial oxidation state of the metallic species occurs, resulting in the desorption of the metal from the surface of the  $TiO_2$ . Equation 3 supports the above in the case of Cr:

$$\operatorname{Cr}(\operatorname{III}) \xrightarrow{h_{VB}^+/\cdot \operatorname{OH}} \operatorname{Cr}(\operatorname{IV}) \xrightarrow{h_{VB}^+/\cdot \operatorname{OH}} \operatorname{Cr}(\operatorname{V}) \xrightarrow{h_{VB}^+/\cdot \operatorname{OH}} \operatorname{Cr}(\operatorname{VI})$$
(3)

In the specific case of Arsenic Figure 5D, the re-oxidation of the metal is lower, and the concentration tends to stabilize after a reactiontime of 3 hours. This may be associated with the oxidation states of this heavy metal, in which its negative valence can contribute to favor the adsorption of the metal on the surface of  $TiO_2$ , which is positively charged due to the acidic pH that occurs in the reaction medium, with values of 2.98 for the drainage under study. This suggests that there would be a synergistic effect between the chemical photoreduction reaction and the physical absorption of the metal on the surface of the semiconductor [24], thus leading to better stability of As.

This ion adsorption effect on the surface of  $TiO_2$  has been evidenced in the fluoridation process, where a low pH must be maintained to favor the impregnation of the strongly electronegative Fluorine on Titania [25–27].

Photocatalysts were also analyzed by Atomic Absorption Spectroscopy after the photocatalytic reaction, and the presence of each metal in the solid phase was found. In the case of As, for example, the final metal content was 3.60, 2.47, 3,40, and 3.42  $\mu$ g/L on commercial  $TiO_2$ , Sg- $TiO_2$ , S- $TiO_2$ , and F- $TiO_2$ , respectively.

The effectiveness for the removal of Fe, Cu, Cr, and As during the first hour of reaction was as follows:  $TiO_2$  (Sigma) > F- $TiO_2$  > S- $TiO_2$  > Sg- $TiO_2$ . The commercial variant of  $TiO_2$  demonstrated a better performance in comparison to the variant produced in the laboratory. Although the Sq- $TiO_2$  material was less effective in the treatment of coal mining drainage, it was possible to observe that by modifying this material through the fluoridation and sulfation processes, it was possible to increase its effectiveness in photocatalytic treatment. These processes have a positive impact on the properties of  $TiO_2$  prepared in the laboratory using the Sol-gel methodology. Fluoridation and sulfation allowed the following improvement possibilities: (a) An increase in the surface area of the  $\operatorname{Sg-}TiO_2$  material (Table 1), leading to a higher surface area available for the reduction of metals on the modified semiconductor which results in greater effectiveness for the removal of metals compared to the starting material. (b) Increased crystallinity of Sq- $TiO_2$  given the presence of the anatase crystalline phase in the material which favors charge transfer during photocatalytic treatment, making it more efficient [13, 14, 28]. (c) An increase in the absorption of the  $\operatorname{Sq-}TiO_2$  material towards the visible region of the electromagnetic spectrum (Figure 3), which leads to a greater ability to use light during photocatalysis.

Despite the positive physicochemical characteristics obtained with the  $\operatorname{Sg-}TiO_2$  material through the addition of fluoride and sulfate ions, it was not possible to obtain a material that would be more effective than commercial  $TiO_2$  for the removal of heavy metals. This can be explained by considering that the grain size of the commercial material is smaller compared to the other analyzed materials. Since photocatalysis is a phenomenon that takes place on the surface [25], it is convenient that the particle size of the semiconductor is smaller, as shown in the current study. Similarly, the lower effectiveness of the sulfonated and fluorinated material prepared in the laboratory can be attributed to possible double obstruction of the active sites [29] on the surface of the  $TiO_2$  derived from the presence of sulfate and fluoride ions found in the material, added to the high concentration of sulfates

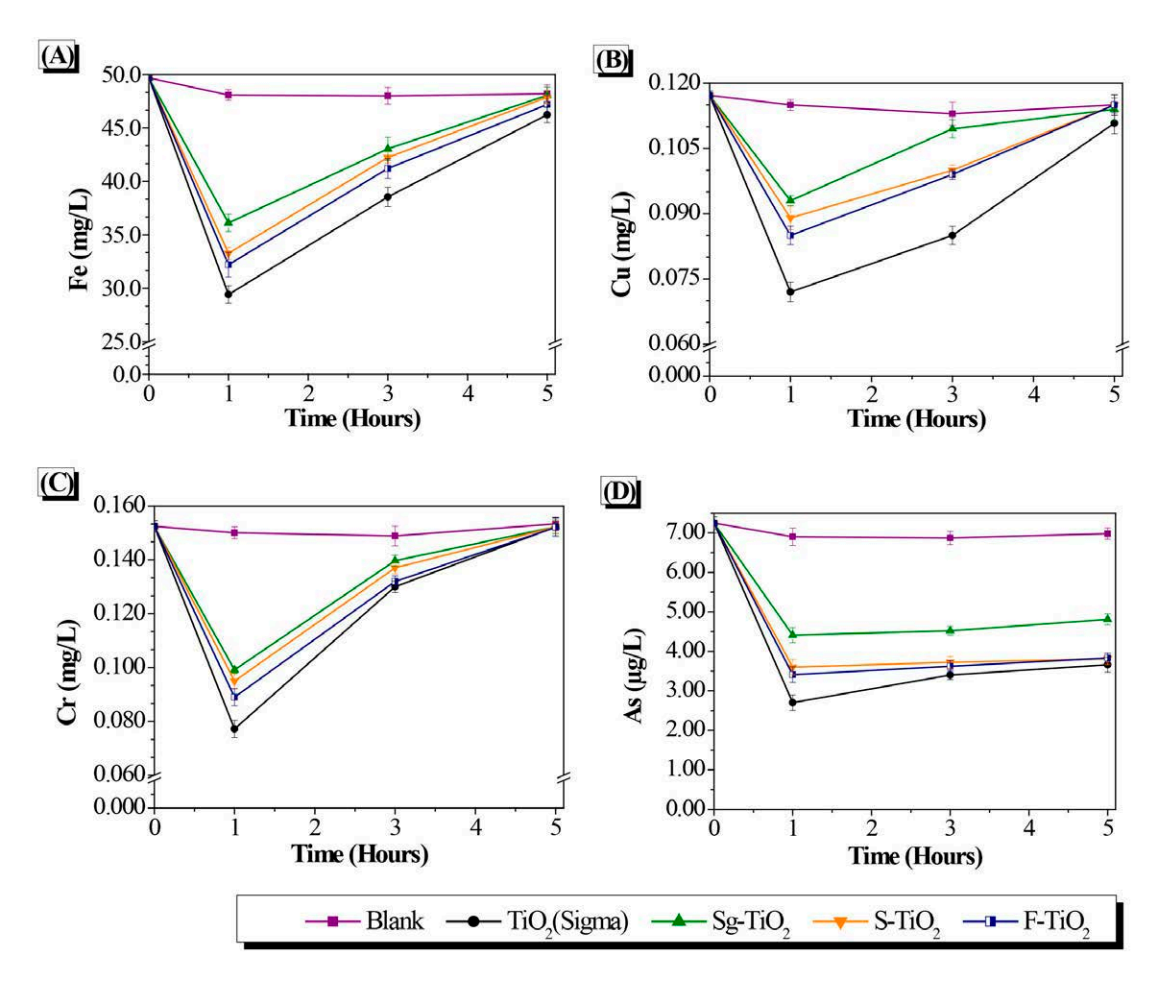


Figure 5 Evolution of the concentration of (A) Fe, (B) Cu, (C) Cr, and (D) As in the coal mining drainage, as a function of the

present in the treated sample (Table 2).

#### Removal of Pb and Ni

The results of monitoring the change in the concentration of Pb and Ni as a function of the photocatalytic reaction time are presented in Figure 6.

The effect of UV-Vis light on the control treatment is small compared to the reduction of these metals. However, when adding the photocatalyst material to the reaction medium, a very significant decrease in the concentration of Pb and Ni is observed in the drainage under study. Unlike what was observed for the metals evaluated in the previous section (Fe, Cu, Cr, and As), the concentration of Pb and Ni, decreased during the first 3 hours of the reaction. The reduction of both Pb and Ni is much more stable on the surface of the semiconductors with respect to the other metals, whose reduction is only stable during the first hour of the photocatalytic reaction (Figure 5). After 3 hours of the reaction, the re- oxidation of Pb and Ni begins to take place, as evidenced by the

increase in their concentration in the reaction medium.

The most effective material for the removal of Pb and Ni from the coal mining drainage was the  $TiO_2$  synthesized in the laboratory (Sq- $TiO_2$ ), and not the commercial material as presented in the case of the other metals. This behavior can be explained by the conclusions from Rajeshwar et al. [30], which suggest possible routes for the photocatalytic removal of metal ions. Both  ${
m Pb}^{2+}$  and Ni<sup>2+</sup> are examples of metals that are reduced indirectly, meaning that they are capable of being reduced by the effect of reducing radicals, not by a direct effect of the electrons of the conduction band as previously thought. In addition to the reduction process, the oxidation process of metals can also take place through the holes  $(h^+)$  in the valence band (VB) or •OH radicals. The process that occurs for the oxidation of metals is described in Equation 4.

$$M^{n+} + h^{+} / \cdot OH \rightarrow M^{(n+1)+} + {}^{-}OH$$
 [4]

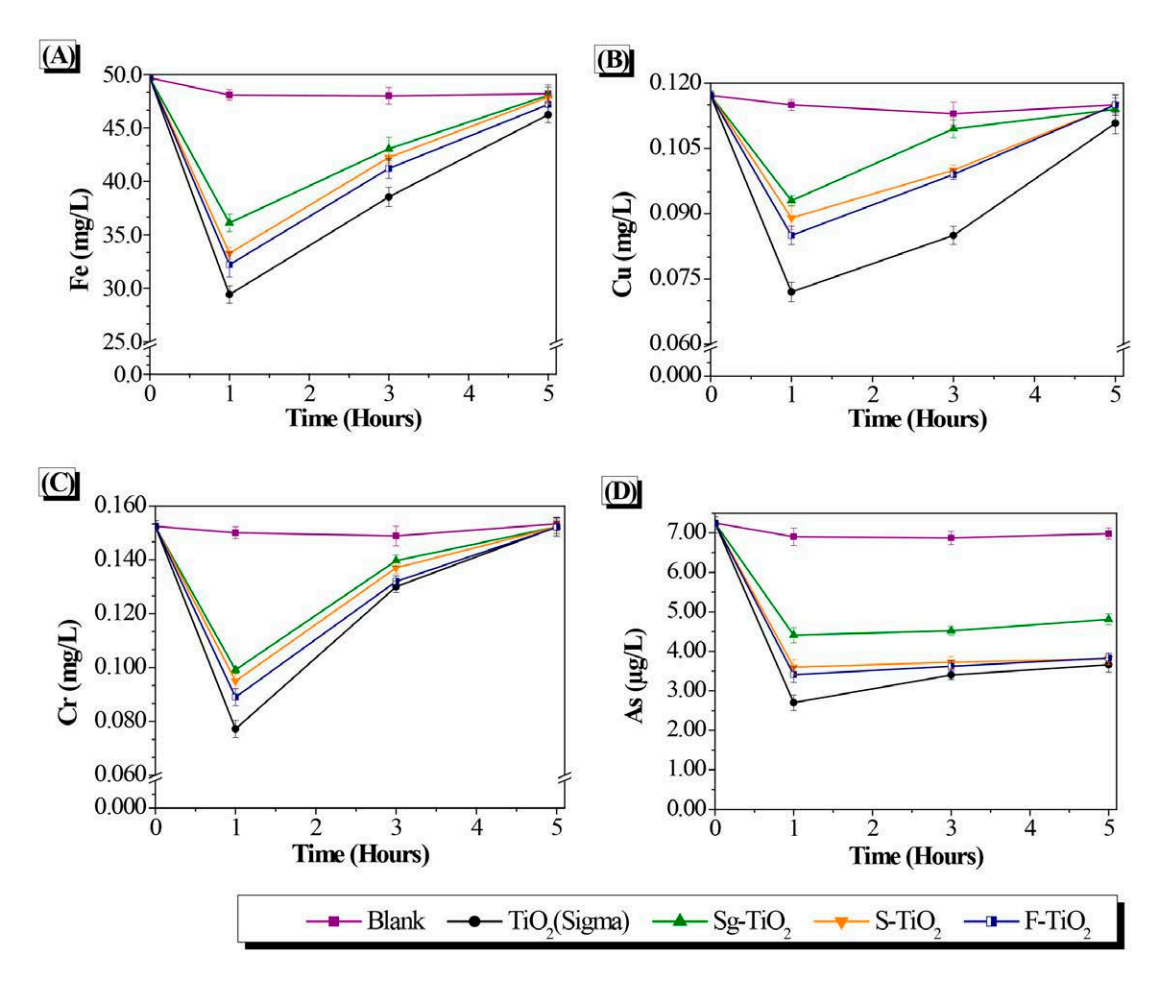


Figure 6 Evolution of the concentration of (A) Pb and (B) Ni in the coal mining drainage, as a function of the photocatalytic treatment time

#### **Removal of anions**

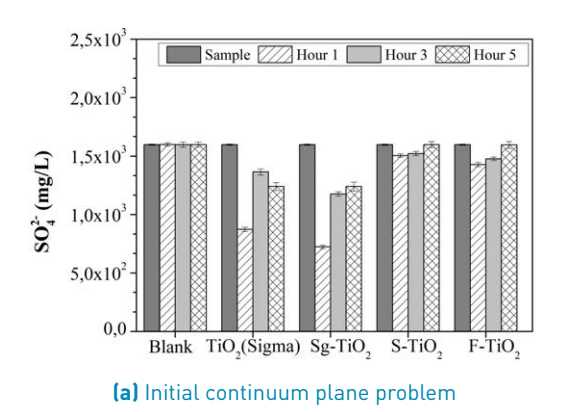
The results of the removal of sulfates and sulfides from the coal mine drainage are presented in Figure 7. In the control reaction, no effect from UV-Vis light was found in the removal of these anions and their initial concentration did not change even after 5 hours of treatment. However, the presence of photocatalysts in the reaction medium did lead to a decrease in the concentration of anions in the fluid phase.

The addition of sulfate ions on the surface of  $TiO_2$  prepared in the laboratory is a viable alternative for modifying the surface properties of this oxide, given the effectiveness of the adsorption of these ions on its surface [31, 32]. The photocatalytic treatment also allows the removal of sulfates and sulfides from the coal mining drainage, which remained adsorbed on the surface of the  $TiO_2$ . In general, the highest removal of these anions was found when the  $Sg\text{-}TiO_2$  material was used in the treatment, which decreased the concentration of Sulfates and Sulfides in the fluid phase in a proportion of 54.7% and 45.6%, respectively, during the first hour of the reaction.

The difference in the removal of the anions under study between the use of commercial and laboratory prepared  $TiO_2$  was very small and may fall within experimental error. However, when comparing the behavior of the material prepared in the laboratory with that of the materials obtained after modifying them by sulfation and fluoridation, it is evident that the effectiveness in removing sulfates and sulfides is much higher.

This can be explained by taking into account that  $\operatorname{Sg-}TiO_2$  presents a surface that is more available to the adsorption of the polluting anions present in the coal mining drainage and can take place more effectively when compared to modified materials that are previously loaded with sulfate and fluoride ions from the synthesis process.

Despite the effectiveness presented by this treatment and similar to that observed for the metals previously studied, it was found that after the third hour of treatment, the concentration of these anions tended to return to the initial values presented by the original sample. This can be caused by competition for the semiconductor surface,



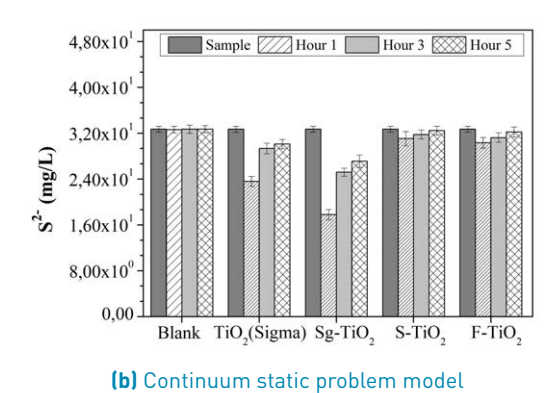


Figure 7 Change in the concentration of (A)  $SO_4^2$  and (B)  $S^2$  in the coal mining drainage, as a function of the photocatalytic treatment time

which is generated between anions, metal ions, and other contaminants present in the drainage.

It is important to mention that the presence of chloride ions was also detected in the coal mining drainage in trace concentrations. There was no observed change in the concentration of these anions during or after the photocatalytic treatment with any of the evaluated materials.

#### **Organic Pollutants**

The concentration of phenolic compounds was monitored, and Figure 8 shows that there is a decrease in the concentration of these pollutants in the course of treatment with the different photocatalytic materials.

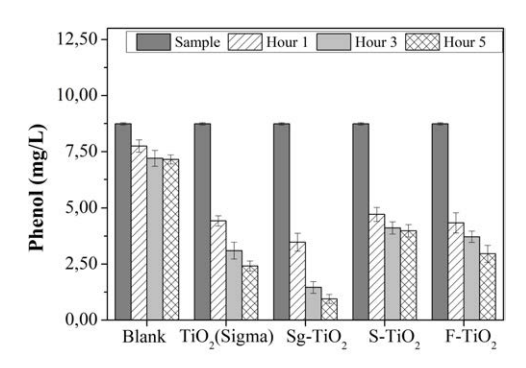


Figure 8 Change in the phenol concentration in the coal mining drainage as a function of photocatalytic treatment time

The greatest effectiveness in the photodegradation of phenolic compounds was achieved with  $TiO_2$  prepared in the laboratory, followed by that obtained with a commercial oxide. In general, fluoridation and sulfation have been reported to be effective mechanisms to obtain a titanium dioxide that is more active and effective in the photocatalytic removal of organic pollutants [15, 20, 33].

However, the current study found that the materials  $\mathrm{S-}TiO_2$  and  $\mathrm{F-}TiO_2$  are less effective for the removal of phenolic compounds in coal mining drainage, which is not in accordance with what is classically reported in the literature. It must be noted that most studies refer to samples prepared in the laboratory and that in most cases, they involve solutions of a single contaminant. The current study dealt with samples from real industrial drainages where the content and type of pollutants were very high and variable.

By taking into account that the photodegradation of phenol is determined by the adsorption of this substrate on the surface of the  $TiO_2$ , these factors put the photocatalytic treatment under real working conditions to the test. This is important because there is a competition of pollutants for OH radicals that can be generated, thus reducing the effectiveness of the materials that were initially thought to be highly efficient for a particular type of pollutant.

During the photocatalytic process, different redox reactions take place and there is the possibility that during this treatment process, more potentially toxic organic compounds may be generated than the compounds present in the initial industrial drainage [34, 35]. It is very important to establish if the organic pollutants present in the wastewater under treatment are undergoing a photocatalytic process of complete mineralization (production of  $CO_2$  and water) or if reaction intermediates are being generated. A very useful tool to establish if this phenomenon occurs is the TOC analysis. current study using the TOC analysis, an average content of 32.2 mg/L was found in the initial mining drainage. After the photocatalytic treatments using the different materials under study, an average value of 32.1 mg/L was found, indicating that this parameter does not decrease significantly. The result obtained indicates that during the photocatalytic treatment, there is little elimination of organic compounds and that complete mineralization

of the same is taking place without the production of reaction intermediates that may be potentially more toxic. According to the observed results, it can be concluded that the chemical photoreduction of metals is the reaction that takes place preferentially on the surface of the photocatalysts evaluated, reducing the effectiveness of the process of elimination of other anions or organic pollutants.

#### 4. Conclusions

Despite the improvement of the physicochemical characteristics obtained in the Sq- $TiO_2$  material through the addition of fluoride and sulfate ions, it was not possible to obtain a more effective material than commercial  $TiO_2$ for the removal of Fe, Cu, Cr, and As. This was explained by taking into account that the grain size of the commercial material was smaller compared to the other analyzed materials which favored greater effectiveness. Contrary to the above,  $\operatorname{Sg-}TiO_2$  achieved slightly better results in the removal of Pb and Ni, with respect to the series of the other photocatalysts tested for the treatment of drainage, especially given that the prepared material presented a greater surface hydroxylation compared to commercial  $TiO_2$ . Apart from the observed phenomena, it was also possible to adsorb polluting anions (sulfides and sulfates) on the surface of the evaluated photocatalysts present in the coal mining drainage especially since the Sq- $TiO_2$ had a surface which was less inhibited in comparison to materials modified on the surface. This allowed a greater removal of these contaminants from the fluid phase.

Using TOC analysis and phenol concentration analysis to determine the mineralization of organic compounds during the photocatalytic treatment determined no significant elimination of these pollutants. Therefore, it could be concluded that under the experimental conditions stated, the chemical photoreduction of metals was the reaction that was carried out preferentially on the surface of the photocatalysts analyzed in the treatment of coal mining drainage.

From the study, it is possible to conclude that the best experimental conditions for the treatment of drainage from the coal industry are provided using commercial  $TiO_2$  as a photocatalyst, a maximum reaction time of 1 hour, using a radiation intensity of 120 W/m2, constant stirring, and under a continuous nitrogen flow.

The experimental results concluded that photocatalysis is a non-selective remediation technology that allows the simultaneous treatment of different types of contaminating species present in composite samples. These results are considered to be preliminary in the search for a potentially more efficient photocatalytic material for the treatment

of inorganic and organic contaminants in a real industrial liquid matrix.

## 5. Declaration of competing interest

We declare that we have no competing interests, including financial or non-financial, professional, or personal interests interfering with the full and objective presentation of the work described in this manuscript.

## 6. Acknowledgments

Ceidy Geraldine Patiño-Castillo would like to thank Gobernación de Boyacá for the award of a MSc researcher grant.

We are grateful to the staff of the Facultad Seccional Sogamoso of Universidad Pedagógica y Tecnológica de Colombia for their extensive help and for use of their excellent laboratory facilities. We are particularly grateful to Jhonathan Andrés Díaz A, Mónica del Pilar Alfonso P, Inés Vergara G. and Mercedes Díaz L. for field and laboratory assistance.

## 7. Funding

This work was supported and financed by the Fondo Nacional de Financiamiento para la Ciencia, la Tecnología e Innovación (FCTel) del Sistema general de regalías (Award No. 733 for the training of high-level human resources of the department of Boyacá and Minciencias) and by Universidad Pedagógica y Tecnológica de Colombia.

#### 8. Author contributions

Julie Joseane Murcia-Mesa: Conceptualization, methodology, supervision, and funding acquisition. Ceidy Geraldine Patiño-Castillo: Investigation and data processing. Hugo Alfonso Rojas-Sarmiento: Funding acquisition and project administration. José Antonio Navío-Santos: Photocatalysts characterization. María del Carmen Hidalgo-López: Photocatalysts characterization. Alberto Angel-Botero: Physicochemical analysis of coal mining drainage.

## 9. Data availability statement

The authors confirm that the data supporting the findings of this study are available within the article [and/or] its supplementary materials.

## **References**

- [1] D. B. Johnson and K. B. Hallberg, "Acid mine drainage remediation options: a review," *Science of The Total Environment*, vol. 338, no. 1-2, Feb. 1, 2005. [Online]. Available: https://doi.org/10.1016/j. scitotenv.2004.09.002
- [2] P. Singer and W. Stumn, "Acidic mine drainage: The rate-determining step," *Science*, vol. 167, no. 3921, Feb. 20, 1970. [Online]. Available: http://doi:10.1126/science.167.3921.1121.
- [3] A. S. Sheoran and V. Sheoran, "Heavy metal removal mechanism of acid mine drainage in wetlands: A critical review," *Minerals Engineering*, vol. 19, no. 2, Feb. 2006. [Online]. Available: https://doi.org/10.1016/j.mineng.2005.08.006
- [4] M. Barakat, "New trends in removing heavy metals from industrial wastewater," *Arabian Journal of Chemistry*, vol. 4, no. 4, Oct. 2011. [Online]. Available: https://doi.org/10.1016/j.arabjc.2010.07.019
- [5] M. Litter, "Heterogeneous photocatalysis: Transition metal ions in photocatalytic systems," *Applied Catalysis B: Environmental*, vol. 23, no. 2-3, Nov. 1, 1999. [Online]. Available: https://doi.org/10.1016/ S0926-3373(99)00069-7
- [6] C. Wang and et al., "Photocatalytic cr(vi) reduction in metal-organic frameworks: A mini-review," Applied Catalysis B: Environmental, vol. 193, Sep. 15, 2016. [Online]. Available: https://doi.org/10.1016/j. apcatb.2016.04.030
- [7] E. Wahyuni, N. Aprilita, H. Hatimah, A. Wulandari, and M. Mudasir, "Removal of toxic metal ions in water by photocatalytic method," *Chemical Science International Journal*, vol. 5, no. 2, 2015. [Online]. Available: https://doi.org/10.9734/ACSJ/2015/13807.
- [8] T. Zhang, X. Wang, and X. Zhang, "Recent progress in tio<sub>2</sub>-mediated solar photocatalysis for industrial wastewater treatment," *International Journal of Photoenergy*, vol. 2014, Jul. 8, 2014. [Online]. Available: https://doi.org/10.1155/2014/607954
- [9] J. Murcia, M. Hidalgo, J. Navío, J. Araña, and J. Doña-Rodríguez, "Study of the phenol photocatalytic degradation over tio<sub>2</sub> modified by sulfation, fluorination, and platinum nanoparticles photodeposition," *Applied Catalysis B: Environmental*, vol. 179, Dic. 2015. [Online]. Available: https://doi.org/10.1016/j.apcatb.2015.05. NAO
- [10] H. Park and W. Choi, "Effects of tio<sub>2</sub> surface fluorination on photocatalytic reactions and photoelectrochemical behaviors," *The Journal of Physical Chemistry B*, vol. 108, no. 13, Mar. 9, 2004. [Online]. Available: https://doi.org/10.1021/jp036735i
- [11] L. Bridgewater, A. P. H. Association, A. W. W. Association, and W. E. Federation, Standard Methods for examination of water and wastewater, 22nd ed., E. Rice, R. Baird, A. Eaton, and L. Clesceri, Eds. Washington, USA: American Public Health Association, 2012.
- [12] Y. R. Park and K. J. Kim, "Structural and optical properties of rutile and anatase tio<sub>2</sub> thin films: Effects of co doping," *Thin Solid Films*, vol. 484, no. 1-2, Jul. 22, 2005. [Online]. Available: https://doi.org/10.1016/j.tsf.2005.01.039
- [13] N. Nolan, M. Seery, and S. Pillai, "Spectroscopic investigation of the anatase-to-rutile transformation of sol-gel-synthesized tio<sub>2</sub> photocatalysts," *The Journal of Physical Chemistry C*, vol. 113, no. 36, Sep. 2009. [Online]. Available: https://doi.org/10.1021/jp904358g
- [14] F. Amano and et al., "Decahedral single-crystalline particles of anatase titanium(iv) oxide with high photocatalytic activity," Chemistry of Materials, vol. 21, no. 13, Jun. 2009. [Online]. Available: https://doi.org/10.1021/cm9004344
- [15] A. Vijayabalan, K. Selvam, R. Velmurugan, and M. Swaminathan, "Photocatalytic activity of surface fluorinated tio<sub>2</sub>-p25 in the degradation of reactive orange 4," *Journal of Hazardous Materials*, vol. 172, no. 2-3, Dic. 30, 2009. [Online]. Available: https: //doi.org/10.1016/j.jhazmat.2009.07.082
- [16] G. Colón and et al., "Structural and surface approach to the enhanced photocatalytic activity of sulfated tio<sub>2</sub> photocatalyst," Applied Catalysis B: Environmental, vol. 63, no. 1-2, Mar. 22, 2006. [Online]. Available: https://doi.org/10.1016/j.apcatb.2005.09.008
- [17] M. Mrowetz and E. Selli, "Enhanced photocatalytic formation of hydroxyl radicals on fluorinated tio2," Physical Chemistry Chemical

- *Physics*, vol. 7, no. 6, Feb. 2, 2005. [Online]. Available: https://doi.org/10.1039/B500194C
- [18] M. Takeuchi, G. Martra, S. Coluccia, and M. Anpo, "Verification of the photoadsorption of h<sub>2</sub>o molecules on tio<sub>2</sub> semiconductor surfaces by vibrational absorption spectroscopy," *The Journal of Physical Chemistry C*, vol. 111, no. 27, Jun. 12, 2007. [Online]. Available: https://doi.org/10.1021/jp0689159
- [19] A. Torrentst and A. Stone, "Catalysis of picolinate ester hydrolysis at the oxide/water interface: inhibition by coadsorbed species," *Environmental Science & Technology*, vol. 27, no. 6, Jun. 1, 1993. [Online]. Available: https://doi.org/10.1021/es00043a004
- [20] M. S. Vohra, S. Kim, and W. Choi, "Effects of surface fluorination of tio<sub>2</sub> on the photocatalytic degradation of tetramethylammonium," *Journal of Photochemistry and Photobiology A: Chemistry*, vol. 160, no. 1-2, Ago. 7, 2003. [Online]. Available: https://doi.org/10.1016/ S1010-6030[03]00221-1
- [21] T. Khoa-Le, D. Flahaut, H. Martinez, T. Pigot, H. K. Hung-Nguyen, and et al., "Surface fluorination of single-phase tio2 by thermal shock method for enhanced uv and visible light induced photocatalytic activity," Applied Catalysis B: Environmental, vol. 144, Jun. 20, 2013. [Online]. Available: https://doi.org/10.1016/j.apcatb.2013.06.027
- [22] N. Serpone, D. Lawless, and R. Khairutdinov, "Size effects on the photophysical properties of colloidal anatase tio<sub>2</sub> particles: Size quantization versus direct transitions in this indirect semiconductor?" The Journal of Physical Chemistry, vol. 99, no. 45, Nov. 1, 1995. [Online]. Available: https: //doi.org/10.1021/j100045a026
- [23] Resolución 631 DE 2015, Diario Oficial No. 49.486 de 18 de abril de 2015, Ministerio de Ambiente y Desarrollo Sostenible, Bogotá, Colombia, 2015.
- [24] M. Mueses and F. Machuca, "Molecular adsorption model for organic compounds over tio<sub>2</sub> - p25 by protonic distribution affinity," *Ingeniería y competitividad*, vol. 15, no. 2, Nov. 2013. [Online]. Available: https://bit.ly/2S6RCn2
- [25] H. Park, Y. Park, W. Kim, and W. Choi, "Surface modification of tio<sub>2</sub> photocatalyst for environmental applications," *Journal* of *Photochemistry and Photobiology C: Photochemistry Reviews*, vol. 15, Jun. 2013. [Online]. Available: https://doi.org/10.1016/j. jphotochemrev.2012.10.001
- [26] J. Yu, W. Wang, B. Cheng, and B. Su, "Enhancement of photocatalytic activity of mesporous tio<sub>2</sub> powders by hydrothermal surface fluorination treatment," *The Journal of Physical Chemistry C*, vol. 113, no. 16, Mar. 31, 2009. [Online]. Available: https: //doi.org/10.1021/jp900136q
- [27] C. Minero, G. Mariella, V. Maurino, and E. Pelizzetti, "Photocatalytic transformation of organic compounds in the presence of inorganic anions. 1. hydroxyl-mediated and direct electron-transfer reactions of phenol on a titanium dioxide-fluoride system," *Langmuir*, vol. 16, no. 6, Ene. 21, 2000. [Online]. Available: https://doi.org/10.1021/la9903301
- [28] N. Sugishita, Y. Kuroda, and B. Ohtani, "Preparation of decahedral anatase titania particles with high-level photocatalytic activity," *Catalysis Today*, vol. 164, no. 1, Abr. 30, 2011. [Online]. Available: https://doi.org/10.1016/j.cattod.2010.11.003
- [29] M. Abdullah, G. Low, and R. Matthews, "Effects of common inorganic anions on rates of photocatalytic oxidation of organic carbon over illuminated titanium dioxide," *The Journal of Physical Chemistry C*, vol. 94, no. 17, Ago. 1, 1990. [Online]. Available: https://doi.org/10.1021/j100380a051
- [30] K. Rajeshwar, C. R. Chenthamarakshan, Y. Ming, and W. Sun, "Cathodic photoprocesses on titania films and in aqueous suspensions," *Journal of Electroanalytical Chemistry*, vol. 538-539, Dic. 13, 2002. [Online]. Available: https://doi.org/10.1016/ S0022-0728[02]00902-6
- [31] G. Colón, M. Hidalgo, J. Navío, A. Kubacka, and M. Fernández, "Influence of sulfur on the structural, surface properties and photocatalytic activity of sulfated tio<sub>2</sub>," *Applied Catalysis B: Environmental*, vol. 90, no. 3-4, Ago. 17, 2009. [Online]. Available: https://doi.org/10.1016/j.apcatb.2009.04.026
- [32] A. V. Vorontsov, H. Valdés, P. G. Smirniotis, and Y. Paz, "Recent

- advancements in the understanding of the surface chemistry in tio<sub>2</sub> photocatalysis," *Surfaces*, vol. 3, no. 1, Feb. 18, 2020. [Online]. Available: https://doi.org/10.3390/surfaces3010008
- [33] J. Kim, W. Choi, and H. Park, "Effects of tio<sub>2</sub> surface fluorination on photocatalytic degradation of methylene blue and humic acid," *Research on Chemical Intermediates*, vol. 36, no. 2, Mar. 10, 2010. [Online]. Available: https://doi.org/10.1007/s11164-010-0123-8
- [34] S. Malato, P. Fernández, M. Maldonado, J. Blanco, and W. Gernjak, "Decontamination and disinfection of water by solar photocatalysis:
- Recent overview and trends," *Catalysis Today*, vol. 147, no. 1, Sep. 15, 2009. [Online]. Available: https://doi.org/10.1016/j.cattod.2009. 06.018
- [35] I. Konstantinou and T. Albanis, "Tio<sub>2</sub>-assisted photocatalytic degradation of azo dyes in aqueous solution: kinetic and mechanistic investigations: A review," *Applied Catalysis B: Environmental*, vol. 49, no. 1, Abr. 20, 2004. [Online]. Available: https://doi.org/10.1016/j.apcatb.2003.11.010